

## X-Ray Studies of Phonon Softening in TiSe<sub>2</sub>

M. Holt,<sup>1,2</sup> P. Zschack,<sup>2</sup> Hawoong Hong,<sup>2</sup> M. Y. Chou,<sup>3</sup> and T.-C. Chiang<sup>1,2,\*</sup>

<sup>1</sup>*Department of Physics, University of Illinois at Urbana-Champaign, 1110 West Green Street, Urbana, Illinois 61801-3080*

<sup>2</sup>*Frederick Seitz Materials Research Laboratory, University of Illinois at Urbana-Champaign, 104 South Goodwin Avenue, Urbana, Illinois 61801-2902*

<sup>3</sup>*School of Physics, Georgia Institute of Technology, Atlanta, Georgia 30332-0430*

(Received 13 November 2000)

The charge-density-wave transition in TiSe<sub>2</sub>, which results in a commensurate ( $2 \times 2 \times 2$ ) superlattice at temperatures below  $\sim 200$  K, presumably involves softening of a zone-boundary phonon mode. For the first time, this phonon-softening behavior has been examined over a wide temperature range by synchrotron x-ray thermal diffuse scattering.

DOI: 10.1103/PhysRevLett.86.3799

PACS numbers: 63.20.Dj, 05.70.Fh, 61.10.Eq, 64.70.-p

Charge-density waves (CDWs) have been studied extensively for decades, as they provide a rich testing ground for basic concepts in electron-phonon coupling, electron correlation, and structural phase transitions, all of which impact our quest for understanding and design of modern complex functional materials. The most widely investigated CDW systems are the numerous layered transition-metal dichalcogenides [1–3]. Despite the intense effort and widespread interest in these materials, many important effects related to the CDW transitions remain yet to be explored and clarified. This paper reports a study of TiSe<sub>2</sub>, a prototypical layered CDW system which undergoes a CDW transition at  $\sim 200$  K to form a simple commensurate ( $2 \times 2 \times 2$ ) superlattice at low temperatures [1]. At room temperature, neutron-scattering measurements of the phonon dispersion relations show already the presence of a Kohn anomaly for the lowest phonon mode  $L_1^-$  at the Brillouin zone boundary, which presumably softens as the temperature decreases [4–7]. However, this softening behavior has not been observed directly, due in part to a very low neutron cross section. Using the third-generation synchrotron-radiation source at the Advanced Photon Source, we have performed a detailed x-ray scattering study of this system showing that the frequency of the  $L_1^-$  phonon mode does indeed decrease gradually from its room temperature value towards zero at the transition temperature. This Letter thus confirms the soft mode concept, which is central to the theory of the CDW phenomenon in this type of material.

The simplest model for CDW formation involves Fermi surface nesting resulting in an enhanced electron-phonon coupling that drives a lattice distortion [5]. TiSe<sub>2</sub>, however, does not fit into this conventional model because its Fermi surface does not nest. A number of other mechanisms have been proposed and discussed in the literature, including exciton formation due to electron-hole coupling across a narrow gap [8–10], an antiferroelectric transition suppressed by carriers [11], and a band Jahn-Teller effect [1,12]. Until now, this

subject remains highly controversial. The most detailed microscopic theory in existence for this system suggests a band Jahn-Teller effect as the likely explanation [1]. A key feature of this theory is that the  $L_1^-$  phonon frequency, renormalized by a temperature-dependent electronic susceptibility, softens towards the transition temperature. This is in agreement with our finding.

Our experiment was performed at the undulator beam line of Sector 33, operated by the University, Industry, and National Laboratory Collaborative Access Team, at the Advanced Photon Source, Argonne National Laboratory. A single crystal of TiSe<sub>2</sub> was prepared following standard methods [3] and attached to the copper cold finger of a closed-cycle helium refrigerator by thermally conductive grease. The sample assembly was enclosed in a vacuum shroud equipped with a hemispherical Be dome for the x-ray measurements. The temperatures reported below were the readings from a silicon diode attached to the copper cold finger. Incident x-ray radiation was set at 8.1 keV, and the quasielastically scattered radiation was collected using a four-circle diffractometer setup. The incident radiation was sufficiently intense to cause sample heating, and calculations suggested a local temperature rise of the order of 10 K relative to the cold finger. Thus, the apparent transition temperature as measured by the thermocouple would be  $\sim 10$  K below the actual transition temperature.

Figure 1 shows typical scans along an  $A$ - $L$ - $A$  line in  $k$  space at various temperatures. The momentum transfer  $\mathbf{q} \equiv (q_1, q_2, q_3)$  for each scan is constrained such that  $q_1 = \frac{1}{7}$ ,  $q_2$  varies linearly between  $-0.65$  and  $-0.35$ , and  $q_3 = \frac{1}{2}$ . The observed intensity variation is derived from thermal diffuse scattering (scattering by thermally populated phonons). Within the adiabatic limit, the line shape is given by [13]

$$I(\mathbf{q}) \propto \sum_{j=1}^9 \frac{|F_j(\mathbf{q})|^2}{\omega_j(\mathbf{q})} \coth\left(\frac{\hbar\omega_j(\mathbf{q})}{2k_B T}\right), \quad (1)$$

where the phonon structure factor  $F$  is given by

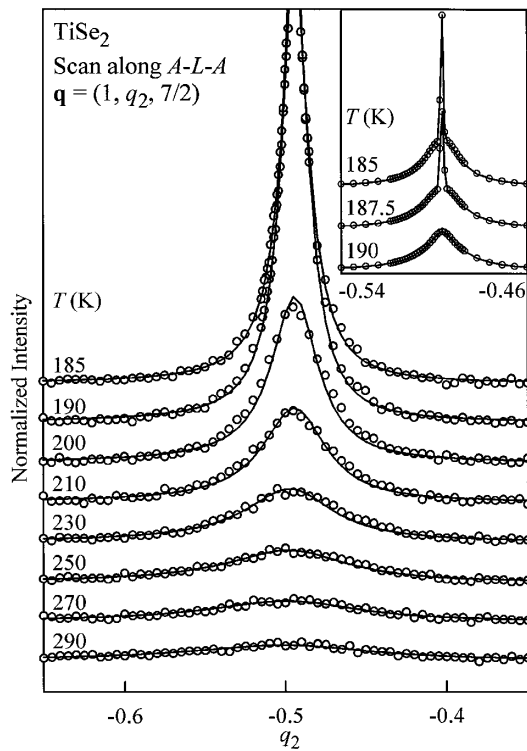


FIG. 1. Linear scans of x-ray thermal diffuse scattering along an  $A$ - $L$ - $A$  line in reciprocal space.  $q_2 = -\frac{1}{2}$  corresponds to an  $L$  point. The sample temperature is indicated for each scan. The inset contains additional scans taken with a finer  $k$  resolution and displayed with a reduced vertical scale to show the emergence of a Bragg peak at  $L$  below the transition temperature.

$$F_j(\mathbf{q}) = \sum_{n=1}^3 f_n(\mathbf{q}) \exp[-M_n(\mathbf{q}) - i\mathbf{q} \cdot \boldsymbol{\tau}_n] \frac{\mathbf{q} \cdot \hat{\mathbf{e}}_{n,j}(\mathbf{q})}{\sqrt{\mu_n}}. \quad (2)$$

In the above equations,  $n$  is an atomic index in a basis consisting of one Ti atom and two Se atoms,  $j$  is an index for the nine phonon branches, and  $f$ ,  $M$ ,  $\boldsymbol{\tau}$ ,  $\mu$ ,  $\omega$ , and  $\hat{\mathbf{e}}$  stand for the atomic scattering factor, the Debye-Waller factor, the atomic position vector in the basis, the atomic mass, the phonon frequency, and the phonon polarization vector, respectively. The phonon structure factor is a smooth, slowly varying function. The hyperbolic cotangent function represents the phonon population including the zero-point vibration, which, together with the remaining  $1/\omega$  factor, favors heavily the lowest phonon branch ( $j = 1$ ). Thus, a large scattering intensity corresponds to a small  $\omega_1$ , and vice versa. It is straightforward to show that  $I \propto \omega_1^{-2}$  in the limit of a small  $\omega_1$  at the  $L$  point.

In Fig. 1, one can clearly see a peak at  $q_2 = -\frac{1}{2}$ , which corresponds to the  $L$  point in the Brillouin zone. This thermal diffuse peak is weak and broad near room temperature. It narrows and intensifies as the temperature decreases. The inset shows additional scans with a reduced intensity scale. As  $T$  decreases below  $T_c = 189$  K, a

resolution-limited Bragg peak emerges with an intensity increasing as  $1 - (T/T_c)^2$  in accordance with the prediction of a Landau theory for a normal-to-lock-in phase transition [14]. Simultaneously, the thermal diffuse peak reaches a maximum intensity at  $T_c$ , and diminishes at lower temperatures. Shown in Fig. 2 is the measured diffuse scattering intensity at the  $L$  point as a function of  $T$ , which appears to diverge at  $T_c = 189$  K. Moving off the  $L$  point, the diffuse intensity still peaks at  $T_c = 189$  K, but the peaking becomes more rounded and diminishes farther away from the  $L$  point.

In Fig. 1, the peaking of the thermal diffuse intensity at  $L$  at room temperature is due to the aforementioned Kohn anomaly. As the dispersion of the lowest phonon branch bends downward near the  $L$  point, the reduced  $\omega_1$  at  $L$  gives rise to the peaking. Upon cooling, thermal diffuse scattering should generally decrease due to a reduction of the phonon population. However, the results in Fig. 1 are clearly opposite to this trend. This can be attributed to a gradual reduction of  $\omega_1$ . Such mode softening leads to an increased phonon population, despite the lowering temperature, as well as an increased cross section through the  $1/\omega$  factor. Thus, the net result is an increased diffuse intensity near  $L$  as  $T$  approaches  $T_c$  from above. This intensity increase at  $L$ , shown in Fig. 2, obeys approximately a  $(T - T_c)^{-1}$  power law.

The intensity variations as a function of  $T$  and momentum transfer  $q_2$ , shown in Fig. 1, are analyzed using Eqs. (1) and (2) and a force constant model for the lattice dynamics. All force constants have been determined previously from a fit to the available neutron data at room temperature [15]. One of the force constants can be related to the softening [7,15], and this is employed as a fitting parameter for scans at various temperatures. The only other parameters are a constant background representing higher order, defect, and stray scattering for each scan, and an overall intensity normalization factor. The fits, shown in Fig. 1 as solid curves, are excellent. Not only is the

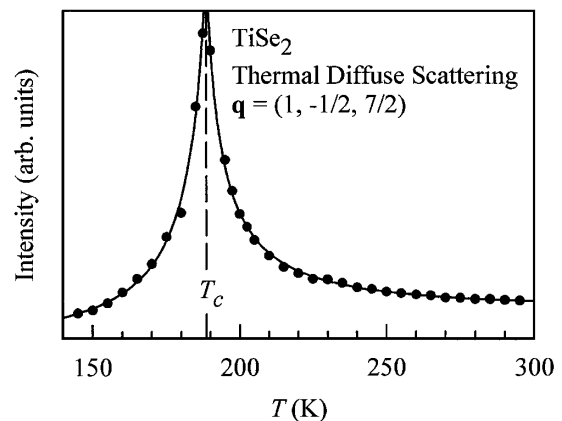


FIG. 2. Thermal diffuse scattering intensity at  $L$  as a function of temperature (the Bragg peak has been subtracted off). The circles are data points, and the curves are just a guide to the eye.

intensity variation well reproduced, so is the line shape change (narrowing as  $T$  decreases towards  $T_c$ ). All of this is achieved with the adjustment of just one force constant.

The force constant resulting from the fit yields the phonon dispersion curves shown in the left panel of Fig. 3. The upper eight phonon branches are independent of temperature, while the lowest branch softens near the  $L$  point as  $T$  decreases towards  $T_c$ . The right panel of Fig. 3 shows an amplified view of the variation of this dispersion curve as a function of temperature. A Kohn anomaly is clearly present at room temperature, and becomes more pronounced towards lower temperatures. At  $T_c$ , the  $L_1^-$  frequency becomes zero, and a static lattice distortion sets in to form a  $(2 \times 2 \times 2)$  superlattice. This static distortion increases in amplitude as  $T$  decreases, giving rise to an increasingly more intense Bragg peak as seen in Fig. 1.

Figure 4 shows the frequency of the  $L_1^-$  mode derived from our analysis. The solid circles represent data points above  $T_c$ , while the open circles are results obtained from the same analysis of the thermal diffuse peak with the Bragg peak ignored. These open circles, connected by a dashed curve as a guide to the eye, do not correspond to any physical frequency, because the lattice is already statically distorted. The system now has different crystal symmetry and a different dynamic matrix. We nevertheless include these fitting results in the figure to show the sharp change at  $T_c$ . The shape of the curve for  $T$  slightly below  $T_c$  should still be meaningful by analytic continuation. The cusp in the curve allows us to pinpoint the transition temperature, which is in perfect agreement with the observed first appearance of a Bragg peak. The solid curve in Fig. 4 for  $T > T_c$  is a fit using the expansion

$$\omega(T) = \sqrt{T - T_c} [a + b(T - T_c) + c(T - T_c)^2], \quad (3)$$

where  $T_c = 188.7$  K,  $a = 7.92 \times 10^{-2}$ ,  $b = 2.40 \times 10^{-4}$ , and  $c = 1.91 \times 10^{-6}$  are fitting parameters. The  $\sqrt{T - T_c}$  prefactor dominates the temperature dependence near the critical point, and can be derived from a Landau theory. The data, however, cover a wide range of temperature, and a second-order polynomial expansion is needed to account for higher-order effects. The dashed curve for  $T < T_c$  is a fit using an expression similar to Eq. (3), except that the prefactor is replaced by  $\sqrt{T_c - T}$  based on the same Landau theory, and a cubic polynomial expansion is employed. A detailed analysis for  $T < T_c$  must involve a  $(2 \times 2 \times 2)$  dynamic matrix, and splitting of phonon modes due to the lowered symmetry makes it a difficult task.

A word of caution is in order. The adiabatic approximation assumed in our analysis could break down for  $T$  near  $T_c$ , resulting in the formation of a central peak that has been the subject of much debate [2,16]. A central peak can be static (caused by sample-dependent impurities and defects) or dynamic (caused by fluctuations which are usually more pronounced in one-dimensional systems), and may appear as a Bragg-like peak above  $T_c$ . The results in Fig. 1 show no evidence for such an effect, and, therefore, this is neglected in our analysis. Another related issue is phason scattering [17], which is important for incommensurate CDW systems and can complicate the analysis substantially.  $\text{TiSe}_2$  is commensurate, and this complication does not arise.

As mentioned in the introduction, the soft-mode concept is central to many theories of structural phase transitions. For  $\text{TiSe}_2$ , this predicted soft-mode behavior has never been observed directly by neutron scattering because of the lack of signal strength. With the advent

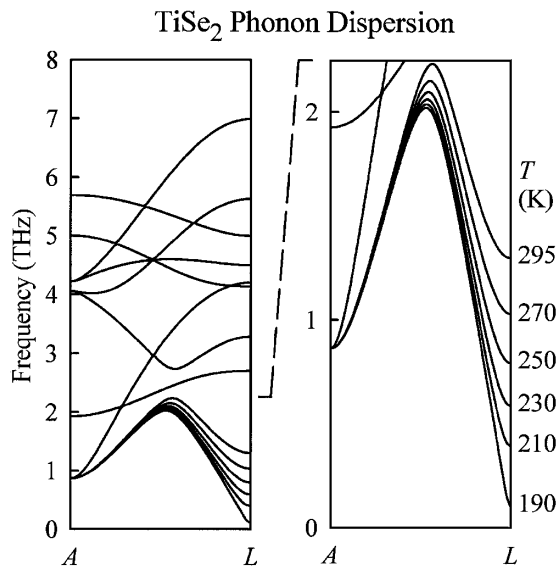


FIG. 3. Phonon dispersion curves of  $\text{TiSe}_2$  as a function of temperature deduced from x-ray diffuse scattering. The lowest phonon branch softens as the temperature decreases towards the transition temperature.

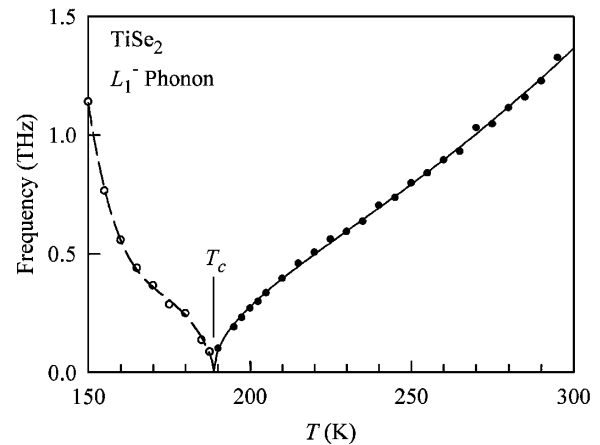


FIG. 4. The filled circles represent experimentally deduced frequency of the  $L_1^-$  phonon mode as a function of temperature. The open circles are results from the same analysis with the Bragg peak ignored. The curves are fits to the data.

of third-generation synchrotron radiation sources, phonon studies under conditions unfavorable to traditional neutron-scattering measurements become accessible. Our results clearly show the soft-mode behavior, and verify key features of this phase transition, including the characteristic power laws for the phonon frequency and the intensity variations near  $T_c$ . These results provide confirmation of theoretical concepts that have remained untested until now. This work also illustrates the power of x-ray scattering and the kinds of new opportunities enabled by high-intensity third-generation synchrotron radiation sources for materials research.

This work is supported by the U.S. Department of Energy (Division of Materials Sciences, Office of Basic Energy Sciences) under Grants No. DEFG02-ER9645439 (T.C.C., Frederick Seitz Materials Research Laboratory, University of Illinois at Urbana-Champaign) and No. DE-FG02-97ER45632 (M.Y.C., Physics, Georgia Institute of Technology). The UNICAT facility at the Advanced Photon Source (APS) is supported by the University of Illinois, Frederick Seitz Materials Research Laboratory (U.S. Department of Energy, the State of Illinois-IBHE-HECA, and the National Science Foundation), the Oak Ridge National Laboratory (U.S. Department of Energy under contract with University of Tennessee-Battelle LLC), the National Institute of Standards and Technology (U.S. Department of Commerce), and UOP LLC. The APS is supported by the U.S. Department of Energy, Basic Energy Sciences, Office of Science, under Contract No. W-31-109-ENG-38. Acknowledgments are also made to the Donors of the Petroleum Research Fund, administered by the American Chemical Society, and to the National Science Foundation Grants No. DMR-99-75182 and No. 99-75470 (T.C.C.) for partial equipment support in connection with the synchrotron beam line operation.

\*Email address: t-chiang@uiuc.edu

- [1] *Structural Phase Transitions in Layered Transition Metal Compounds*, edited by K. Motizuki (Reidel, Boston, 1986).
- [2] *Charge Density Waves in Solids*, edited by L. P. Gor'kov and G. Grüner (North-Holland, New York, 1989).
- [3] J. A. Wilson and A. D. Yoffe, *Adv. Phys.* **18**, 193 (1969).
- [4] W. G. Stirling, B. Dorner, J. D. N. Cheeke, and J. Revelli, *Solid State Commun.* **18**, 931 (1976).
- [5] F. J. DiSalvo, D. E. Moncton, and J. V. Waszczak, *Phys. Rev. B* **14**, 4321 (1976).
- [6] D. E. Moncton, F. J. DiSalvo, and J. D. Axe, in *Proceedings of the International Conference on Lattice Dynamics*, edited by M. Balkanski (Flammarion, Paris, 1978), p. 561.
- [7] N. Wakabayashi, H. G. Smith, K. C. Woo, and F. C. Brown, *Solid State Commun.* **28**, 923 (1978).
- [8] J. A. Wilson, *Phys. Status Solidi (b)* **86**, 11 (1978).
- [9] W. Kohn, *Phys. Rev. Lett.* **19**, 439 (1967).
- [10] Th. Pillo, J. Hayoz, H. Berger, F. Lévy, L. Schlapbach, and P. Aebi, *Phys. Rev. B* **61**, 16 213 (2000).
- [11] R. M. White and G. Lucovsky, *Nuovo Cimento Soc. Ital. Fis.* **38B**, 280 (1977).
- [12] H. P. Hughes, *J. Phys. C* **10**, L319 (1977).
- [13] M. Y. Chou and M. Choi, *Phys. Rev. Lett.* **84**, 3733 (2000); M. Holt and T.-C. Chiang, *Phys. Rev. Lett.* **84**, 3734 (2000). We use a dynamic matrix that is periodic in the reciprocal space.
- [14] K. C. Woo, F. C. Brown, W. L. McMillan, R. J. Miller, M. J. Schaffman, and M. P. Sears, *Phys. Rev. B* **14**, 3242 (1976).
- [15] S. S. Jaswal, *Phys. Rev. B* **20**, 5297 (1979).
- [16] *Dynamic Critical Phenomena and Related Topics*, edited by C. P. Enz (Springer-Verlag, New York, 1979); R. N. Bhatt and W. L. McMillan, *Phys. Rev. B* **12**, 2042 (1975).
- [17] Y. R. Wang and A. W. Overhauser, *Phys. Rev. B* **39**, 1357 (1989); W. Minor, L. D. Chapman, S. N. Ehrlich, and R. Colella, *Phys. Rev. B* **39**, 1360 (1989).